BMC Medical Genomics

RESEARCH

Open Access

Functional analysis of a novel nonsense *PPP1R12A* variant in a Chinese family with infantile epilepsy

Ling Tong[1†], Xinxin Wang[1†], Huiqin Wang[1], Rong Yang[1], Xiaoyan Li[1] and Xiaoguang Yin[1*]

Abstract

Background Defects in *PPP1R12A* can lead to genitourinary and/or brain malformation syndrome (GUBS). GUBS is primarily characterized by neurological or genitourinary system abnormalities, but a few reported cases are associated with neonatal seizures. Here, we report a case of a female newborn with neonatal seizures caused by a novel variant in *PPP1R12A*, aiming to enhance the clinical and variant data of genetic factors related to epilepsy in early life.

Methods Whole-exome and Sanger sequencing were used for familial variant assessment, and bioinformatics was employed to annotate the variant. A structural model of the mutant protein was simulated using molecular dynamics (MD), and the free binding energy between PPP1R12A and PPP1CB was analyzed. A mutant plasmid was constructed, and mutant protein expression was analyzed using western blotting (WB), and the interaction between the mutant and PPP1CB proteins using co-immunoprecipitation (Co-IP) experiments.

Results The patient experienced tonic-clonic seizures on the second day after birth. Genetic testing revealed a heterozygous variant in *PPP1R12A*, NM_002480.3:c.2533 C > T (p.Arg845Ter). Both parents had the wild-type gene. MD suggested that loss of the C-terminal structure in the mutant protein altered its structural stability and increased the binding energy with PPP1CB, indicating unstable protein–protein interactions. On WB, a low-molecular-weight band was observed, indicating that the protein was truncated. Co-IP indicated that the mutant protein no longer interacted with PPP1CB, indicating an effect on the structural stability of the myosin phase complex.

Conclusion The *PPP1R12A* c.2533 C > T variant may explain the neonatal seizures in the present case. The findings of this study expand the spectrum of *PPP1R12A* variants and highlight the potential significance of truncated proteins in the pathogenesis of GUBS.

Keywords *PPP1R12A*, Neonatal seizures, Truncated protein, PP1C, Western blotting

[†]Ling Tong and Xinxin Wang contributed equally to this work.

*Correspondence:
Xiaoguang Yin
ahfyyinxiaoguang@163.com
[1]Department of Neonatology, Anhui Women and Children's Medical Center, No. 15, Yimin Street, Hefei 230001, Anhui, China

Introduction

Seizures are among the most common neurological emergencies in neonates, with an incidence of 1–5‰ among live births [1]. Most neonatal seizures are associated with acute brain injuries, such as hypoxic-ischemic encephalopathy, which accounts for approximately 40% of neonatal seizure cases [1]; however, only a fraction of these cases meet the criteria for a diagnosis of epilepsy or epileptic syndrome. Thus, establishing etiology is crucial for clinical decision-making and precise treatment [2, 3].

With the widespread adoption of next-generation sequencing technologies, the contribution of genetic defects to neonatal seizures is being increasingly recognized. In a prospective cohort study by Shellhaas et al., 58% (34/58) of neonatal seizures were associated with genetic variations [4]. *KCNQ2* variants are commonly associated with neonatal seizures and exhibit a wide phenotypic spectrum ranging from self-limiting seizures, benign familial neonatal, 1 (OMIM#121200) to intractable developmental and epileptic encephalopathy 7 (OMIM#613720) [5]. Other pathological genes include *STXBP1*, *SCN2A*, *ARX*, and *SLC25A22*, which can lead to various forms of neonatal seizures or epileptic syndromes [6–9]. Novel genes associated with neonatal seizures are continuously being identified.

PPP1R12A encodes myosin phosphatase target subunit 1 (MYPT1), which plays a critical role in regulating cell motility and maintaining cellular morphology [10]. Variants in this gene have been linked to genitourinary and/or brain malformation syndrome (GUBS, OMIM#618820), a recently reported syndrome characterized by abnormalities in the nervous system and genitourinary reproductive system [11]. To date, only 13 cases of GUBS have been reported worldwide, and these patients may present with isolated clinical phenotypes of the nervous system, the genitourinary reproductive system, or both [11, 12]. Most patients with GUBS exhibit features, such as agenesis of the corpus callosum or severe cerebral malformations, often accompanied by varying degrees of seizures or spasm episodes [11]. Because patients carrying *PPP1R12A* variants are rare, the spectrum of neurological diseases in GUBS and the underlying pathogenic mechanisms remain poorly understood.

Here, we report the case of a female newborn who presented with severe neonatal seizures. The patient experienced frequent generalized tonic seizures on the second day after birth. Whole-exome sequencing of the family suggested a heterozygous variant in the *PPP1R12A* gene in the patient. In-vitro functional experiments suggested that this variant affected the structural stability of the myosin phase complex. This study highlights the pivotal role of genetic testing in diagnosing the etiology of neonatal seizures and sheds light on how *PPP1R12A* variants may contribute to neonatal seizures.

Materials and methods

Study subjects

The patient was a female newborn who was admitted to our hospital in March 2022. Ethical approval for medical research involving this patient was granted by the ethics committee of our hospital. The parents of the patient provided informed consent and agreed to the disclosure of their child's clinical data, imaging materials, and genetic data. All procedures were conducted in accordance with the 1964 Helsinki Declaration.

Whole-exome sequencing and variant analysis

To genetically analyze the patient's clinical presentation, 3-mL peripheral blood samples were collected from the patient and her parents. Genomic DNA was extracted using a DNA extraction kit (Qiagen, Hilden, Germany), per the manufacturer's instructions. Sequencing libraries were constructed using xGEN® Exome Research Panel v2.0 probes (Integrated DNA Technologies, IA, USA). High-throughput parallel genome sequencing was carried out using the second-generation NovaSeq 6000 sequencing platform (Illumina, CA, USA). Low-quality reads were filtered out and high-quality data (Q30 quality score > 90%) were retained. The reads were aligned to a human reference genome sequence (hg19) using the Burrows–Wheeler Aligner (http://bio-bwa.sourceforge.net) tool. Variant detection was performed using Genome Analysis Toolkit software v3.5 (https://gatk.broadinstitute.org/hc/en-us). Variants of low quality (depth of coverage < 10× and allele fraction < 30%) were excluded. The variants identified were aligned to the NM_002480.3 NCBI reference sequence using Chromas v2.33 software to determine their positions. Multiple variant frequency databases (1000 Genomes, https://www.internationalgenome.org/; Exome Aggregation Consortium [ExAC] East Asian, http://exac.broadinstitute.org; and Genome Aggregation Database [gnomAD] exome East Asian, http://gnomad.broadinstitute.org/) were used to classify the variants according to the guidelines of the American College of Medical Genetics and Genomics (ACMG) [13, 14].

Sanger sequencing

The variant was amplified and sequenced using an ABI 3500 analyzer (Applied Biosystems, USA). The forward primer sequence was 5′-TCAGGCCTACAATCAAGGACCAG-3′ and the reverse primer sequence was 5′-CCCCTAGATAGTCCCCTGGC-3′.

Variant protein structure modeling and interaction simulation analysis

The NM_002480.3 MYPT1 protein sequence file was downloaded from the National Library of Medicine database (www.ncbi.nlm.nih.gov/nuccore/NM_002480.3).

Protein physicochemical properties were predicted using the ProtParam platform (https://web.expasy.org/protparam/). The wild-type and mutant MYPT1 proteins were analyzed using the AlphaFold platform (https://alphafold.ebi.ac.uk/). Molecular dynamics (MD) simulations were performed using GROMACS 5.14. The simulations were conducted with the GROMOS53A6 force field for a total duration of 50 ns, and each simulation system was subjected to a 50-ps position-restrained simulation. The root mean square deviation (RMSD) of the proteins was calculated using the gmx rms tool, and RMSD scatter plots were created using Origin v8.5 (OriginLab, Northampton, WA, USA). Protein structures were visualized using PyMOL v2.3 (DeLano Scientific LLC, San Francisco, CA, USA).

Cell culture

HEK293T cells (Shanghai Cell Bank, Shanghai, China) were cultured in Dulbecco's modified Eagle's medium containing 10% fetal bovine serum and 100 μg/mL penicillin (Thermo Fisher Scientific, Waltham, MA, USA) in an incubator at 37 °C with 5% CO_2.

Plasmid construction

Full-length human *PPP1R12A* cDNA (NM_002480.3) was amplified using the Phanta® Max Super-Fidelity DNA Polymerase kit (Vazyme #P505) according to the manufacturer's instructions and cloned into pECMV-3×FLAG-N through *Hind*III/*Eco*RI restriction enzyme digestion, resulting in the generation of the recombinant plasmid FLAG-PPP1R12A. The Mut Express MultiS Fast Mutagenesis Kit V2 (Vazyme #C215) was used following the manufacturer's instructions to construct the mutant plasmid FLAG-PPP1R12A-Arg845X. The plasmids were subjected to Sanger sequencing to ensure sequence accuracy (the primer sequences are provided in Supplementary Material 1). HEK293T cells were transfected with FLAG-PPP1R12A or FLAG-PPP1R12A-Arg845X using Lipofectamine 3000 (Thermo Fisher Scientific). Protein levels were assessed using western blotting (WB) 48 h post-transfection.

Western blot

Total protein was extracted from HEK293T cells using lysis buffer (Beyotime, Shanghai, China). The proteins were separated using sodium dodecyl sulfate-polyacrylamide gel electrophoresis (SDS-PAGE) and transferred to a polyvinylidene membrane that was blocked with Tris-buffered saline containing 0.05% Tween-20 (Beyotime) and 5% skim milk powder for 2 h. The membrane was probed with primary antibodies (DYKDDDDK Tag [9A3] mouse mAb [Cat# 8146, diluted 1:1000; Cell Signaling Technology, Danvers, MA, USA]) and GAPDH [D4C6R] mouse mAb [Cat# 97166, diluted 1:1000; Cell Signaling Technology]) at 4 °C overnight and then incubated with secondary antibodies (Anti-mouse IgG, HRP-linked [Cat# 7076, diluted 1:5000; Cell Signaling Technology]) at room temperature for 2 h. Protein complexes were visualized using enhanced chemiluminescence (Thermo Fisher Scientific). Bands were analyzed using the ImageJ software v1.46 (NIH, Bethesda, MD, USA). The assay was repeated three times.

Co-immunoprecipitation (Co-IP)

Myc-PPP1CB (2 μg) was co-transfected with the aforementioned plasmids FLAG-PPP1R12A (2 μg) and FLAG-PPP1R12A Arg845×(2 μg) into HEK293T cells. After 48 h, the cells were washed with phosphate-buffered saline, treated with protein lysis solution, and centrifuged at 20,000 × *g* at 4 °C for 10 min. Three hundred microliters of supernatant was collected and incubated with anti-FLAG immunomagnetic beads (Cat.B26101, Selleck Company) at 4 °C for 2 h. Magnetic beads were washed twice with TBS (50 mM Tris HCl, 150 mM NaCl, pH 7.4). After the addition of 50 μL of protein loading buffer to the precipitate, it was boiled for 5 min, cooled down, and left to stand on a magnetic rack for 1–2 min. The supernatant was subjected to SDS-PAGE detection.

Statistical analysis

Student's *t*-test was used to compare the means of two groups. Graphs were drawn using GraphPad Prism 8 (GraphPad Software, La Jolla, CA, USA).

Results

Patient information

The female neonatal patient was the first child of her mother. The mother underwent a cesarean section delivery at 37+2 weeks of gestation because of fetal intrauterine distress and fetal abdominal fluid accumulation. The infant had a birth weight of 2,740 g, with Apgar scores of 4 at 5 min and 8 at 10 min. After birth, the patient exhibited weak spontaneous breathing, low muscle tone in her limbs, and cyanosis of the extremities. Endotracheal intubation and positive pressure ventilation were initiated for 1 min, which led to improvement, although her spontaneous breathing remained weak. On the second day after birth, the infant experienced tonic-clonic seizures without an identifiable trigger. Her seizures were characterized by clenched fists, upward eye deviation, and an open mouth, with each episode lasting 30–40 s. The patient was treated with phenobarbital and midazolam for seizure control, which reduced seizure frequency. On the seventh day after birth, the infant began to exhibit myoclonic seizures, with each episode lasting 1.5–2 min. Video electroencephalography revealed asynchronous bilateral electrical activity, with generalized sharp waves in the central and occipital regions. Brain magnetic

resonance imaging indicated bilateral cerebral white matter softening, multiple abnormal signals in the bilateral cerebellar hemispheres, and thinning of the corpus callosum (Fig. 1). The father of the infant was 35 years old, and the mother was 34 years old; both were in good health. No consanguinity between the parents or family history of epilepsy were reported.

Identification of a PPP1R12A variant

Whole-exome sequencing revealed a heterozygous variant in *PPP1R12A*, NM_002480.3:c.2533 C>T (p.Arg845Ter), in the affected infant. The variant resulted in a premature termination codon, potentially leading to the formation of a truncated protein. The variant was not reported in the 1000 Genomes, ExAC East Asian, and gnomAD exome East Asian databases. According to the ACMG guidelines, the variant was classified as pathogenic. The basis for this classification included strong

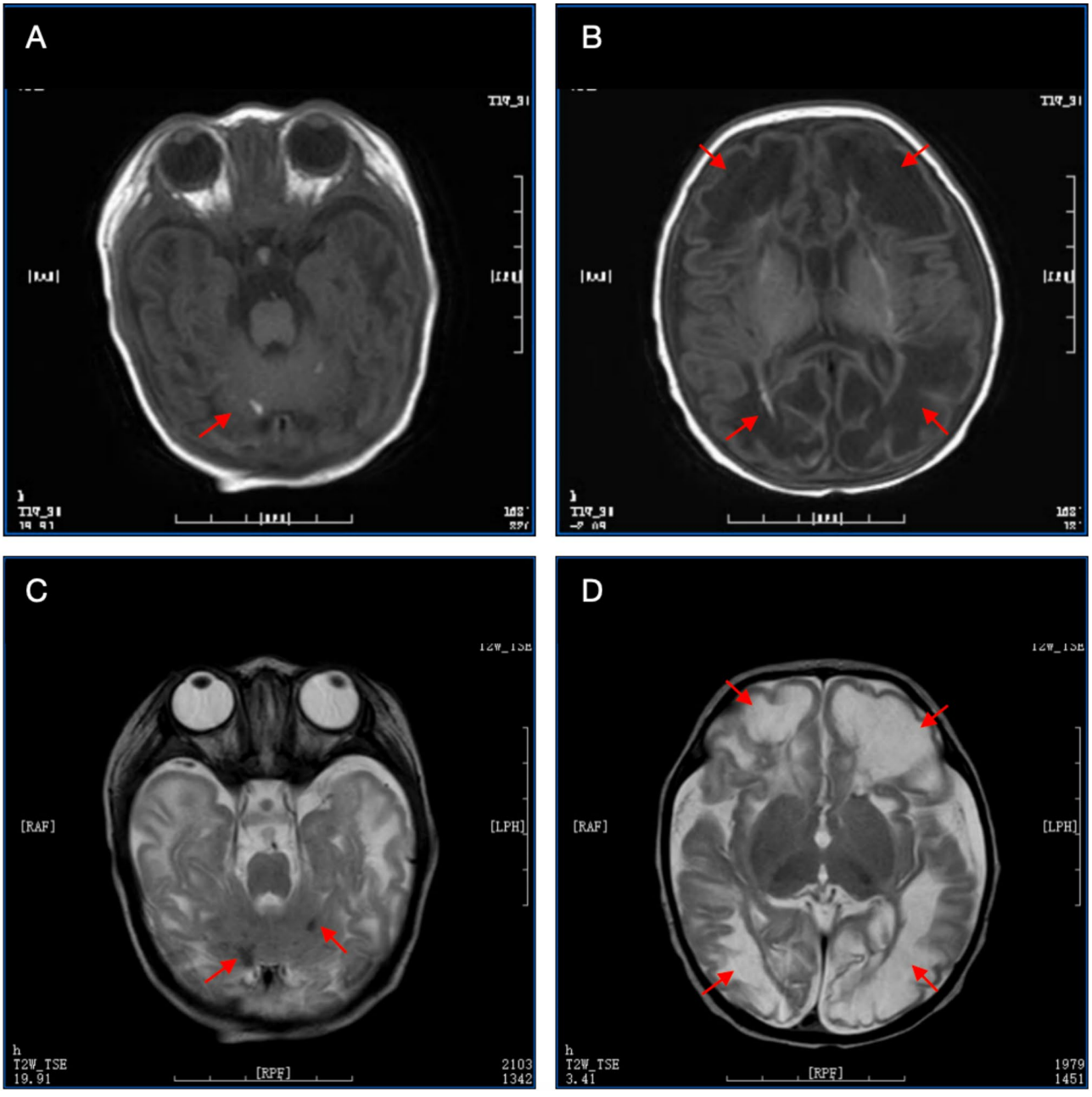

Fig. 1 Brain magnetic resonance imaging of the patient. **A**, **B.** Transverse T1-weighted images showing high-signal lesions in the cerebellum, indicating the possibility of bleeding (**A**) and basal ganglia region, along with multiple cortical softening lesions (**B**). **C**, **D.** Transverse T2-weighted images revealing low signals in the cerebellum and occipital lobe, indicating the possibility of bleeding (**C**) and multiple cortical malacia foci (**D**)

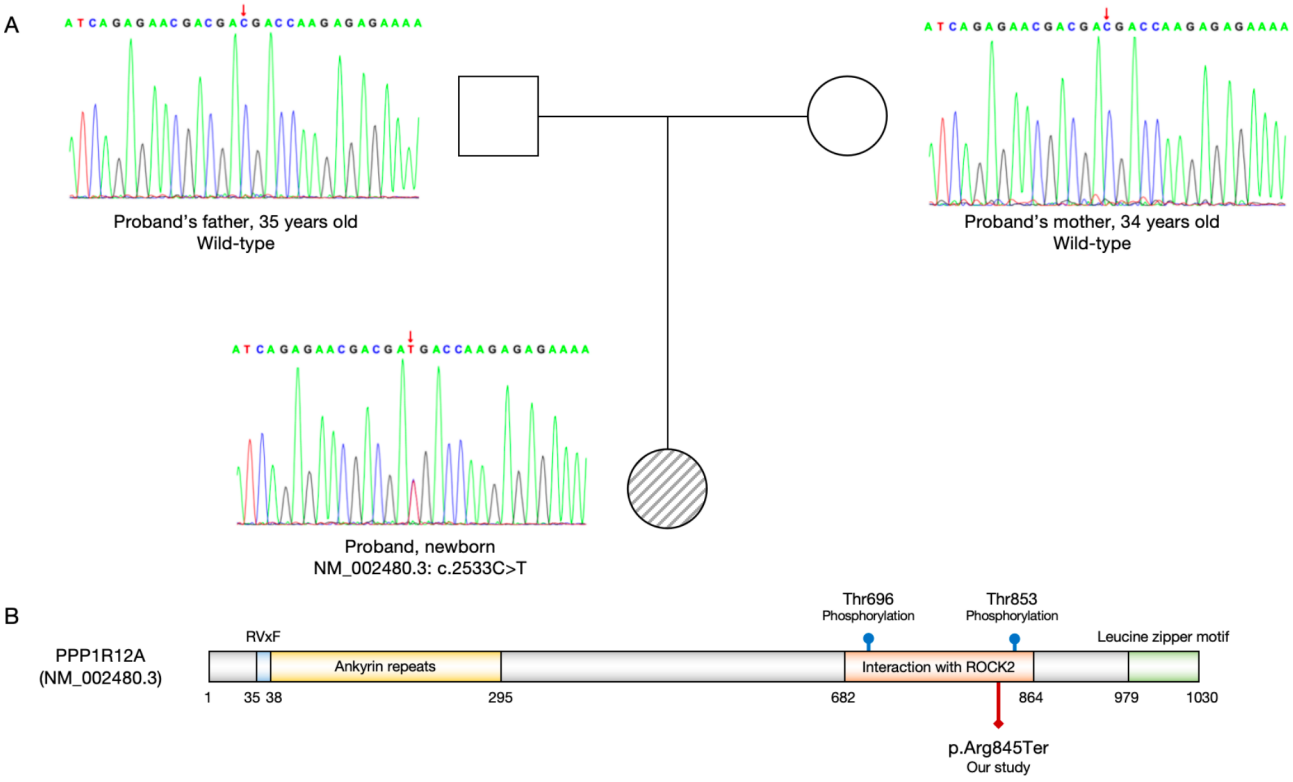

Fig. 2 Genetic variation information of the patient and her parents. **(A)** Sanger sequencing revealed a novel variant in the *PPP1R12A* gene, NM_002480.3:c.2533 C > T, resulting in p.Arg845Ter, in the patient. Both parents had the wild-type gene, suggesting a *de-novo* mutation. **(B)** The PPP1R12A protein consists of structural domains including a (R/K)(V/I)X(F/W) motif (RVxF), adjacent ankyrin repeats, interaction with ROCK2 domain (including Thr696 and Thr853 phosphorylation sites, indicated by blue balls), and a leucine zipper motif. The variant identified in this study is located within the interaction with ROCK2 domain (highlighted by a red arrow)

Table 1 Comparison of general physical parameters between the wild-type and mutant PPP1R12A proteins

	Wild-type PPP1R12A	Mutant PPP1R12A (Arg845Ter)
Amino acids (N)	1030	845
Molecular weight (Da)	115280.71	93560.78
Isoelectric point (PI)	5.31	5.35
Instability index	61.87	64.30
Grand average of hydropathicity	1.055	0.987
Aliphatic index	62.08	62.04

evidence (PVS1) for the presence of a null variant, moderate evidence (PS2_Moderate) from segregation analysis indicating that the variant occurred *de novo*, and supporting evidence (PM2_Supporting) from the absence of the variant in population databases. Sanger sequencing confirmed that the variant was present only in the proband and that both parents had the wild-type gene (Fig. 2).

The truncated protein may lead to reduced structural stability

The wild-type MYPT1 protein consists of 1,030 amino acids and has a molecular weight of 112.5 kDa, whereas the predicted mutant protein is composed of 845 amino acids, with a molecular weight of 91.3 kDa. This finding was corroborated by WB assay results. The mutant protein was predicted to have a slightly reduced hydrophilic index, indicating a decrease in hydrophobicity (Table 1). Protein structural analysis revealed that the wild-type and mutant proteins had equilibrium RMSD values of 0.95 Å and 1.05 Å, respectively. The mutant protein lacked a portion of the C-terminal helical and folded structures, which may have led to reduced protein structural stability (Fig. 3).

The truncated protein may disrupt protein interaction with protein phosphatase 1 catalytic subunit

MYPT1 interacts with protein phosphatase 1 catalytic subunit (PP1C) to form myosin light chain phosphatase (MLCP), which is involved in complex biological functions [15, 16]. In simulations of the interaction between these two proteins, the hydrogen bonds between Gln756 and Arg750 of MYPT1 and Glu167 and Glu56 of PP1C,

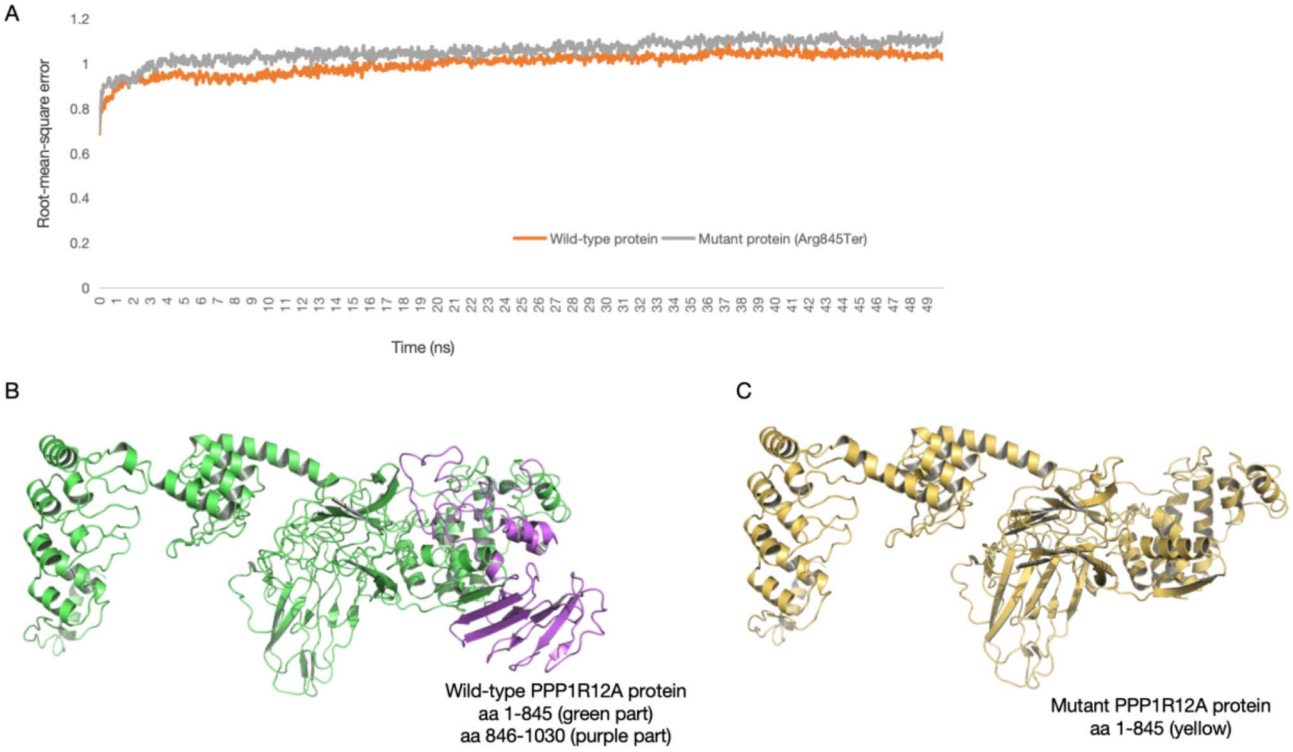

Fig. 3 PPP1R12A protein model. **(A)** MD simulation of the PPP1R12A protein structure. RMSD data for wild-type and mutant proteins over 50 ns. **(B)** PPP1R12A protein model (aa 1–1030). **(C)** Mutant protein model showing the lack of folded and helical structures in the C-terminus of the truncated protein

respectively, were disrupted in the interaction with the mutant protein (Fig. 4). Analysis of the free binding energy between the proteins indicated that the binding energy of the mutant complex was increased by ~50% compared to that of the wild-type complex, suggesting reduced structural stability of the MLCP complex formed by the mutant protein (Table 2).

The variant may produce a truncated protein

FLAG-tagged wild-type (pECMV-PPP1R12A) and mutant (pECMV-PPP1R12A-Arg845X) proteins were expressed in HEK293T cells. WB results revealed significant increases in protein expression from both plasmids compared to the empty vector, suggesting successful protein expression. No significant difference was observed in protein expression from the two plasmids ($p=0.43$). Quantitative analysis revealed the production of a truncated protein with a molecular weight of 96 kDa from the mutant plasmid (Fig. 5A; images of uncut membranes are provided in Supplementary Material 2).

The interaction between the mutant protein and PPP1CB is disrupted

Based on the above structural modeling results, it was predicted that the free binding energy between the mutant and PPP1CB proteins would be reduced, which may interfere with the structural stability of the myosin phase complex. In Co-IP, the input samples yielded the expected bands. FLAG-PPP1R12A and Myc-PPP1CB IP produced a normal band, whereas FLAG-PPP1R12A-Arg845X and Myc-PPPP1CB IP yielded no band, indicating that interaction between the mutant PPP1R12A and PPP1CB proteins was abrogated. This was consistent with the structural modeling results (Fig. 5B; images of uncut membranes are provided in Supplementary Material 3).

Discussion

We described the clinical characteristics of a neonatal patient with epilepsy for whom molecular genetic testing revealed a variant in *PPP1R12A*, c.2533 C>T, (p.Arg845Ter), which had not been previously reported, classifying it as a novel variant. In-vitro experiments suggested that the variant does not affect protein expression but produces a smaller, truncated protein. To elucidate the structural features of the truncated protein, we conducted MD simulations, which indicated that the variant protein has a looser conformation. Furthermore, binding models with the PPP1CB protein suggested that the stability of the variant complex is reduced. Co-IP results confirmed that this mutation may affect the interaction with PPP1CB, thereby affecting the biological function of the myosin phase complex.

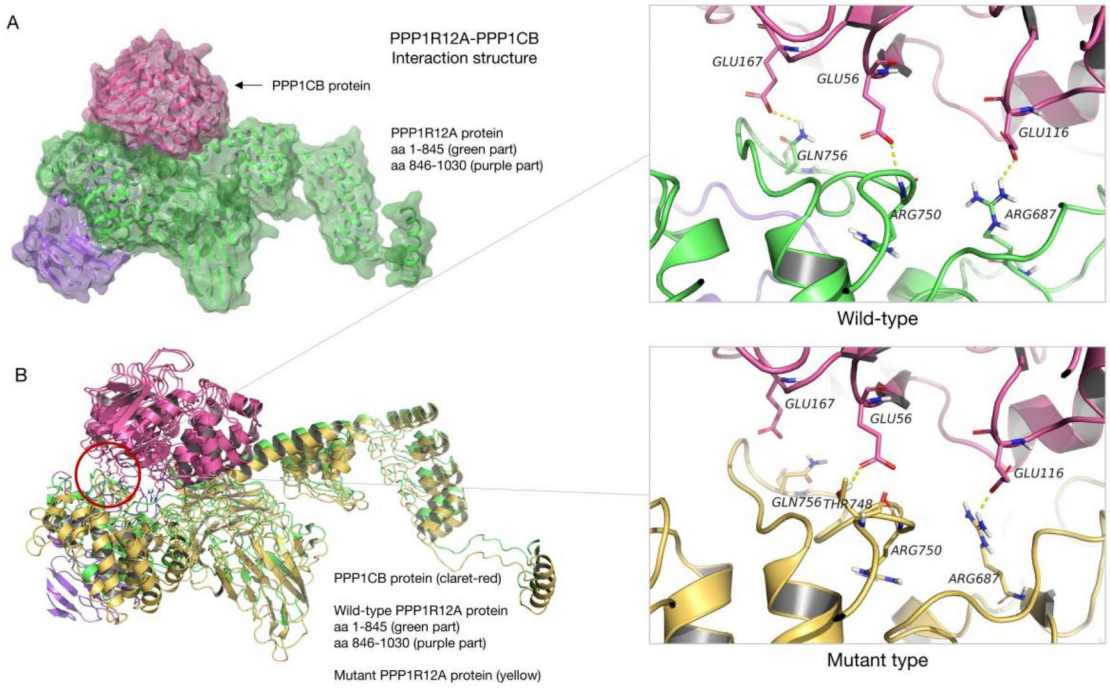

Fig. 4 Structural illustration of the interaction between PPP1R12A and PPP1CB. **(A)** The structure displays the lacking C-terminal portion of PPP1R12A (purple) that does not directly interact with PPP1CB but primarily binds to the N-terminal structure. **(B)** Partial loop structures of PPP1R12A interact with PPP1CB. In the wild-type structure, PPP1R12A residues (Gln756, Arg750, and Arg687) form hydrogen bonds with PPP1CB residues (Glu167, Glu56, and Glu116). In the mutant structure, these hydrogen bonds are disrupted and a new hydrogen bond is formed between PPP1R12A Thr748 and PPP1CB Glu56

Table 2 Changes in the free energy of binding between PPP1R12A and PP1C proteins

Contributors	PPP1R12A (wild-type)–PP1C binding energy (kJ/mol)	PPP1R12A (Arg845Ter)–PP1 binding energy (kJ/mol)
△van der Waals interaction energy	−187.02 ± 1.24	−105.12 ± 1.87
△electrostatic energy	−29.08 ± 0.22	−29.77 ± 0.54
△polar solvation energy	76.69 ± 1.26	78.19 ± 1.22
△non-polar solvation energy	−31.23 ± 0.96	−28.19 ± 0.43
△binding free energy	−170.64 ± 1.26	−84.89 ± 1.88

Among the 13 reported GUBS cases, phenotypic characteristics vary widely and mutations are distributed across multiple exons, making it challenging to establish clear genotype–phenotype correlations [11]. Patients can present neurological phenotypes, genitourinary anomalies, or an overlapping combination of both. For instance, 10 cases presented genitourinary abnormalities, primarily including underdeveloped external genitalia, reproductive gland abnormalities, and a phenotypic spectrum that ranged from 46,XY sex development disorders to individuals who were chromosomally male but exhibited various genitourinary phenotypes, such as cryptorchidism, streak gonads, ovarian dysgenesis, fusion of the labioscrotal folds, clitoral enlargement, and increased labial rugosity [11, 12]. Eight patients showed neurological abnormalities that were mainly evident as abnormal cranial magnetic resonance imaging findings, such as corpus callosum agenesis or severe alobar holoprosencephaly. In some patients, these brain structural anomalies were associated with intellectual disabilities, attention deficit hyperactivity disorder, and epileptic seizures [11]. Notably, GUBS rarely presents with neurophenotypes in young children, which may be because of the small number of reported cases. However, defects in *PPP1R12A* may result in embryonic Mullerian duct regression defects, leading to earlier expression of genitourinary phenotypes [10]. The patient in the current study initially presented with severe epilepsy during the neonatal period and exhibited brain white matter abnormalities and corpus callosum agenesis characteristics similar to those in previous reports. This observation suggests that *PPP1R12A* may play a role in the pathogenesis of neonatal epilepsy; however, further research is required to expand the phenotypic spectrum of patients and explore the underlying mechanisms.

To date, 18 *PPP1R12A* variants, including eight insertions/deletions, seven nonsense variants, one complex rearrangement, and two intron variants, have been reported, and all of these variants have the potential to

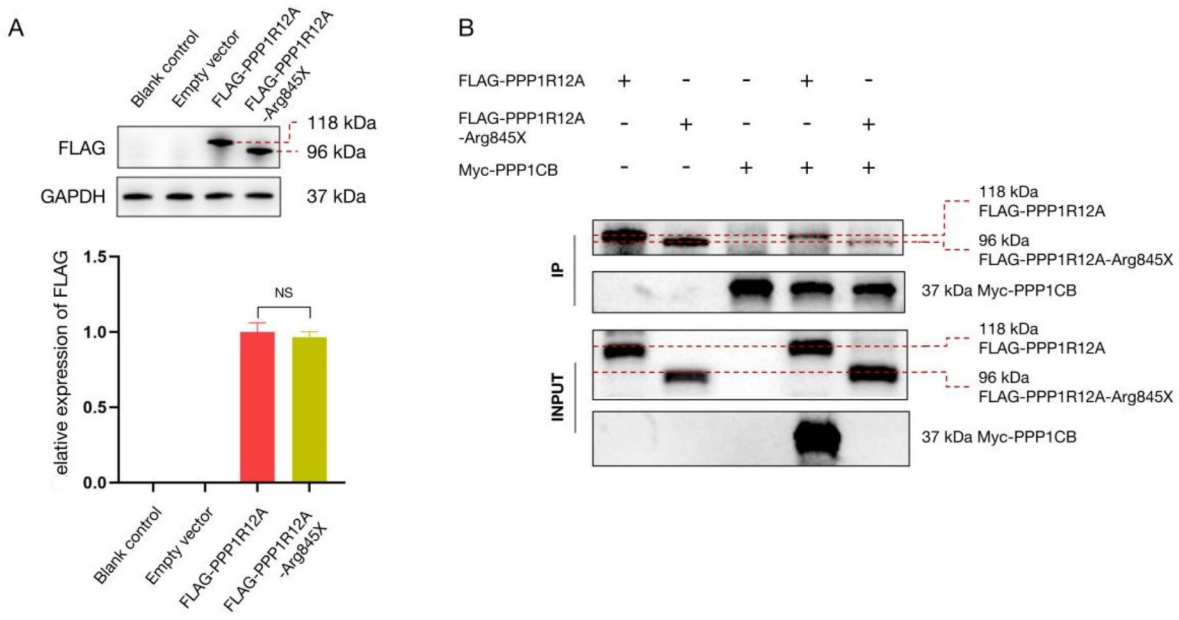

Fig. 5 In-vitro functional analyses. **(A)** WB analysis of N-terminal FLAG-tagged wild-type PPP1R12A (FLAG-PPP1R12A) and variant (FLAG-PPP1R12A-Arg845X) proteins, revealing a decrease in the molecular weight of the variant protein, indicating the generation of a truncated protein. **(B)** Co-IP analysis revealing that Co-IP of FLAG-PPP1R12A-Arg845X with Myc PPP1CB produced no bands, indicating an effect of the mutation on the interaction between these two proteins

result in premature termination of translation of the encoded protein [11, 12]. Hughes et al. suggested that haploinsufficiency of *PPP1R12A* may be a critical factor in human disease phenotypes [11]. However, Okamoto et al. reported that mice with targeted *Ppp1r12a* knockout exhibited embryonic lethality within seven days of conception, and no significant phenotypes were observed in heterozygous knockout mice. This finding suggests that, in addition to haploinsufficiency, *PPP1R12A* defects may be associated with other pathogenic mechanisms [17]. In the present study, the novel variant p.Arg845Ter likely led to the patient exhibiting seizures and brain structural anomalies shortly after birth. Surprisingly, overexpression experiments using a recombinant mutant plasmid revealed the production of a truncated protein. While in-vitro functional experiments did not fully replicate the complex environment in vivo, they suggested the possibility of a truncated protein with reduced biological function. The pathogenic mechanisms of *PPP1R12A* defects remain unclear. This not only reflects the variability of phenotypes among individuals but also suggests potential differences in the mechanisms among different types of variants.

PPP1R12A spans 25 exons and encodes PPP1R12A, also known as MYPT1, a MYPT family member. PPP1R12A is widely expressed in various tissues, including the brain, respiratory system, kidneys, and urinary tract [16]. PPP1R12A, as the regulatory subunit of MLCP, forms a complex with PPP1CB and a 20-kDa protein (M20). MLCP mainly exerts its biological functions by dephosphorylating myosin II light chains, inducing relaxation in smooth muscle and non-muscle tissues [12]. The N-terminal portion of PPP1R12A contains an (R/K)(V/I)X(F/W) motif (RVxF), which is essential for interacting with PPP1CB, exposing more binding regions, such as the ankyrin repeat and acidic regions [18]. The C-terminus has a leucine zipper motif, which interacts with protein kinase G and plays an important role in smooth muscle function [19]. In addition, Rho-kinase can phosphorylate PPP1R12A at Thr696 (or Thr853) near the C-terminal, leading to inhibition of MLCP activity [19]. Furthermore, the C-terminus can interact with M20, the biological function of which remains unclear. Studies have shown that M20 binds to the C-terminal region of PPP1R12A but does not significantly affect phosphatase activity, suggesting that MLCP is mainly a complex of PPP1R12A and PPP1CB [20, 21]. We validated p.Arg845Ter through structural modeling and in-vitro functional experiments The Arg845Ter variant may affect the interaction with PPP1CB. Simultaneously, because of the lack of the key Thr853 site for phosphorylation, this variant may further affect myosin phosphatase enzyme activity.

In summary, we reported a novel *PPP1R12A* variant, p.Arg845Ter, in a neonatal patient with epilepsy that is

likely to encode a truncated protein and may affect protein interaction with PPP1CB. Ultimately, this study expands the spectrum of *PPP1R12A* variants and provides valuable clinical insights into the diagnosis of neurological phenotypes associated with GUBS.

Abbreviations

Co-IP	Co-Immunoprecipitation
IPGUBS	Genitourinary and/or brain malformation syndrome
MLCP	Myosin light chain phosphatase
MYPT1	Myosin phosphatase target subunit 1
PP1C	Protein phosphatase 1 catalytic subunit
WB	Western blotting

Supplementary Information

The online version contains supplementary material available at https://doi.org/10.1186/s12920-024-02009-z.

Supplementary Material 1

Supplementary Material 2

Supplementary Material 3

Author contributions

LT, XW, XY: article topic, concept, and design. LT, RY, XL: conducted the experiments, collected the data, and edited the manuscript. LT, XW, HW: wrote and edited the manuscript and analyzed and interpreted the data. All authors substantially contributed to the study.

Funding

This study was supported by Hefei Municipal Health Commission Medical Application Project (No. HWK2021zd015).

Data availability

No datasets were generated or analysed during the current study.

Declarations

Ethics approval and consent to participate

This work was approved by the Research Ethics Committee of the Anhui Women and Children's Medical Center according to the World Medical Association Declaration of Helsinki. Written informed consent was obtained from the patient's legal guardians.

Consent for publication

Not applicable.

Competing interests

The authors declare no competing interests.

Conflict of interest

The authors declare that they have no known competing financial interests or personal relationships that could have appeared to influence the work reported in this paper.

Received: 20 December 2023 / Accepted: 10 September 2024
Published online: 27 September 2024

References

1. Ziobro J, Shellhaas RA. Neonatal seizures: diagnosis, etiologies, and management. Semin Neurol. 2020;40(2):246–56. https://doi.org/10.1055/s-0040-1702943.
2. Malone A, Ryan CA, Fitzgerald A, Burgoyne L, Connolly S, Boylan GB. Interobserver agreement in neonatal seizure identification. Epilepsia. 2009;50(9):2097–101. https://doi.org/10.1111/j.1528-1167.2009.02132.x.
3. Scheffer IE, Berkovic S, Capovilla G, Connolly MB, French J, Guilhoto L, et al. ILAE classification of the epilepsies: position paper of the ILAE Commission for Classification and terminology. Epilepsia. 2017;58(4):512–21. https://doi.org/10.1111/epi.13709.
4. Shellhaas RA, Wusthoff CJ, Tsuchida TN, Glass HC, Chu CJ, Massey SL, et al. Profile of neonatal epilepsies: characteristics of a prospective US cohort. Neurology. 2017;89(9):893–9. https://doi.org/10.1212/WNL.0000000000004284.
5. Miceli F, Soldovieri MV, Weckhuysen S, Cooper E, Taglialatela M et al. KCNQ2-Related Disorders. [updated 2022 May 19]. In: Adam MP, Feldman J, Mirzaa GM, Pagon RA, Wallace SE, Bean LJH. GeneReviews® [Internet]. Seattle (WA): University of Washington, Seattle; 1993–2023.
6. Saitsu H, Kato M, Mizuguchi T, Hamada K, Osaka H, Tohyama J, et al. *De novo* mutations in the gene encoding STXBP1 (MUNC18-1) cause early infantile epileptic encephalopathy. Nat Genet. 2008;40(6):782–8. https://doi.org/10.1038/ng.150.
7. Wolff M, Johannesen KM, Hedrich UBS, Masnada S, Rubboli G, Gardella E, et al. Genetic and phenotypic heterogeneity suggest therapeutic implications in SCN2A-related disorders. Brain. 2017;140(5):1316–36. https://doi.org/10.1093/brain/awx054.
8. Kato M, Saitoh S, Kamei A, Shiraishi H, Ueda Y, Akasaka M, et al. A longer polyalanine expansion mutation in the ARX gene causes early infantile epileptic encephalopathy with suppression-burst pattern (Ohtahara syndrome). Am J Hum Genet. 2007;81(2):361–6. https://doi.org/10.1086/518903.
9. Molinari F, Raas-Rothschild A, Rio M, Fiermonte G, Encha-Razavi F, Palmieri L, et al. Impaired mitochondrial glutamate transport in autosomal recessive neonatal myoclonic epilepsy. Am J Hum Genet. 2005;76(2):334–9. https://doi.org/10.1086/427564.
10. Grassie ME, Moffat LD, Walsh MP, MacDonald JA. The myosin phosphatase targeting protein (MYPT) family: a regulated mechanism for achieving substrate specificity of the catalytic subunit of protein phosphatase type 1δ. Arch Biochem Biophys. 2011;510(2):147–59. https://doi.org/10.1016/j.abb.2011.01.018.
11. Hughes JJ, Alkhunaizi E, Kruszka P, Pyle LC, Grange DK, Berger SI, et al. Loss-of-function variants in PPP1R12A: from isolated sex reversal to holoprosencephaly spectrum and urogenital malformations. Am J Hum Genet. 2020;106(1):121–8. https://doi.org/10.1016/j.ajhg.2019.12.004.
12. Diao Y, Sun W, Zhang Z, Zhao B, Chen X. Clinical report and genetic analysis of a neonate with genitourinary and/or brain malformation syndrome caused by a non-coding sequence variant of PPP1R12A. Mol Genet Genomic Med. 2023;5:e2223. https://doi.org/10.1002/mgg3.2223.
13. Richards S, Aziz N, Bale S, Bick D, Das S, Gastier-Foster J. Standards and guidelines for the interpretation of sequence variants: a joint consensus recommendation of the American College of Medical Genetics and Genomics and the Association for Molecular Pathology. Genet Med. 2015;17(5):405–24. https://doi.org/10.1038/gim.2015.30.
14. Tavtigian SV, Greenblatt MS, Harrison SM, Nussbaum RL, Prabhu SA, Boucher KM, et al. Modeling the ACMG/AMP variant classification guidelines as a bayesian classification framework. Genet Med. 2018;20(9):1054–60. https://doi.org/10.1038/gim.2017.210.
15. Khasnis M, Nakatomi A, Gumpper K, Eto M. Reconstituted human myosin light chain phosphatase reveals distinct roles of two inhibitory phosphorylation sites of the regulatory subunit, MYPT1. Biochemistry. 2014;53(16):2701–9. https://doi.org/10.1021/bi5001728.
16. Kiss A, Erdődi F, Lontay B. Myosin phosphatase: unexpected functions of a long-known enzyme. Biochim Biophys Acta Mol Cell Res. 2019;1866(1):2–15. https://doi.org/10.1016/j.bbamcr.2018.07.023.
17. Okamoto R, Ito M, Suzuki N, Kongo M, Moriki N, Saito H, et al. The targeted disruption of the MYPT1 gene results in embryonic lethality. Transgenic Res. 2005;14(3):337–40. https://doi.org/10.1007/s11248-005-3453-3.
18. Tóth A, Kiss E, Herberg FW, Gergely P, Hartshorne DJ, Erdödi F. Study of the subunit interactions in myosin phosphatase by surface plasmon resonance. Eur J Biochem. 2000;267(6):1687–97. https://doi.org/10.1046/j.1432-1327.2000.01158.x.
19. Given AM, Ogut O, Brozovich FV. MYPT1 mutants demonstrate the importance of aa 888–928 for the interaction with PKGIalpha. Am J Physiol Cell Physiol. 2007;292(1):C432–9. https://doi.org/10.1152/ajpcell.00175.
20. Murányi A, Derkach D, Erdodi F, Kiss A, Ito M, Hartshorne DJ. Phosphorylation of Thr695 and Thr850 on the myosin phosphatase target subunit: inhibitory effects and occurrence in A7r5 cells. FEBS Lett. 2005L579(29):6611–5. https://doi.org/10.1016/j.febslet.2005.10.055

21. Hartshorne DJ, Ito M, Erdödi F. Role of protein phosphatase type 1 in contractile functions: myosin phosphatase. J Biol Chem. 2004;279(36):37211–4. https://doi.org/10.1074/jbc.R400018200.